

A miniature tunable quadrature shadow oscillator with orthogonal control

Seangrawee Buakaew, Chariya Wongtaychatham

Department of Electronics Engineering, School of Engineering, King Mongkut's Institute of Technology Ladkrabang, Bangkok, Thailand

Article Info

Article history:

Received Oct 29, 2022

Revised Jan 5, 2023

Accepted Jan 14, 2023

Keywords:

Orthogonal control

Quadrature oscillator

Shadow filter

Shadow oscillator

Transconductance amplifier

ABSTRACT

This article presents a new design of a quadrature shadow oscillator. The oscillator is realized using one input and two outputs of a second-order filter cell together with external amplifiers in a feedback configuration. The oscillation characteristics are controlled via the external gain without disturbing the internal filter cell, following the concept of the shadow oscillator. The proposed circuit configuration is simple with a small component-count. It consists of, two voltage-different transconductance amplifiers (VDTAs) along with a couple of passive elements. The frequency of oscillation (FO) and the condition of oscillation (CO) are controlled orthogonally via the dc bias current and external gain. Moreover, with the addition of the external gain, the frequency range of oscillation can be further extended. The proposed work is verified by computer simulation with the use of 180 nm complementary metal-oxide-semiconductor (CMOS) model parameters. The simulation gives satisfactory results of two sinusoidal output signals in quadrature with some small total harmonic distortions (THD). In addition, a circuit experiment is performed using the commercial operational transconductance amplifiers LM13700 as the active components. The circuit experiment also demonstrates satisfactory outcome which confirms the validity of the proposed circuit.

This is an open access article under the [CC BY-SA](https://creativecommons.org/licenses/by-sa/4.0/) license.



Corresponding Author:

Seangrawee Buakaew

Department of Electronics Engineering, School of Engineering, King Mongkut's Institute of Technology Ladkrabang

Chalong Krung, 1 Alley, Lat Krabang, Bangkok 10520, Thailand

Email: Seangrawee.to@kmitl.ac.th

1. INTRODUCTION

The versatility of a quadrature oscillator is well-known in electrical and electronics applications, signal processing, telecommunications, and instrumentation. In modern communication systems, it plays the role of generating reference signals for quadrature amplitude modulation (QAM), single side-band modulation, orthogonal frequency division multiplexing (OFDM), zero-IF and image-reject receivers. In superheterodyne receivers, quadrature oscillators are required in mixers for shifting signals from one frequency range to another [1]. In the field of measurement, quadrature oscillators is the essence for the demodulation section of capacitive rotary encoders [2] used for position and speed measurement. Quadrature oscillators are also employed as signal generators for phase different detectors in measurement systems [3], [4]. It plays a significant role in vector generators and selective voltmeters as well [5]. Therefore, quadrature oscillator circuits are worth going on research and development. It is seen that various literatures of the topic [3]-[21] have been continuously reported over the years.

Among the reported quadrature oscillators current feedback op-amps (CFOA) are employed as the main active components in the circuits published in [3], [5], [7], [9]. However, there is limitation in such

designs for lack of electronic tunability. Besides, the designs require a lot of passive resistors which is unfavorable in the integrated circuit design. In [4], the quadrature oscillator is implemented by using the second generation current conveyor (CCII) but it still lacks electronic tuning capability. A modern analog device, such as current differencing buffer amplifiers (CDBA), is utilized in several quadrature oscillators [6], [8], [13], [14]. However, the frequency of oscillation (FO) cannot be electronically controlled. To overcome this limitation, several passive resistors are replaced with groups of complementary metal–oxide–semiconductor (CMOS) networks [8], but the linear range of tuning parameters is quite narrow.

The quadrature oscillators previously reported in [15]–[17], consist of operational transresistance amplifiers (OTRAs) and a lot of discrete passive elements. They suffer from the same restriction that the oscillator parameters can be adjusted by only changing the passive-element values. Although there is an attempt to adjust some parameters of the oscillator via a capacitor, the method is rarely used due to the uncertain properties of the capacitor and the effect of parasitic resistors at higher operating frequency causing undesired frequency-imprecision [22]. Furthermore, the recently proposed quadrature oscillators [10]–[12], realized by the second-generation voltage conveyor (VCII) require a large number of passive components, however, the FO cannot be electronically tuned. Meanwhile, the quadrature oscillator in [20] can be electronically adjusted through the intrinsic resistance of CCCII via dc bias current. Similarly, in the quadrature oscillators [18], [19], tuning the filter parameters is via the transconductances but it has the effect on the filter cell.

Recently, the principle to design a filtering circuit known as a shadow filter has been introduced, [23]–[31]. The characteristics of these shadow filters such as the pole frequency and the quality factor, are obtained using a feedback signal from a filter cell and an external amplifier for tuning. With this new approach, tuning the filter parameters is more convenient and effective than the traditional concept. This is beneficial for minor error compensation after the completion of the integrated-circuit manufacturing process [31]. More recently, this concept had been applied in the design of a shadow sinusoidal oscillator reported in [32], [33], [34]. Among these, the circuit in [32] consists of a filter cell with three inputs, one output, and two external amplifiers based on CFOAs which are available on the shelf in the feedback loop. However, the circuit lacks electronic tunability. Then changing the FO is only by varying a passive resistor in the circuit. Besides, the circuit configuration requires a lot of passive resistors which is unsuitable for monolithic fabrication. Furthermore, only one single sinusoidal signal is obtained as the output.

The design of the shadow oscillator in [33], two cells of integrators with a single input and multiple outputs are functioned as the core circuit. Only the amplitude of the current output can be controlled via an external amplifier. However, tuning the FO relies on changing the parameters within the integrator cells. In the quadrature shadow oscillator [34], a circuit is designed by employing positive feedback of a high Q shadow bandpass filter and two external amplifiers. Although the FO and the condition of oscillation (CO) can be electronically controlled, adjustment on both interacts with each other. Moreover, the circuit needs an excessive number of voltage differential transconductances (VDTAs), up to three sections.

In this literature, a novel scheme of quadrature shadow oscillator is realized by active devices called the VDTAs, along with two resistors and two grounded capacitors. A few advantages are achieved as the total count of VDTAs is decreased comparing with the circuit in [34]. Both the FO and the CO can be adjusted by controlling the dc bias current of the external gain and this is not interfering with the filter cell and suiting the nature of being a shadow oscillator. This tuning feature is attractive for fine-tuning applications and compensation. Besides, under the same filter parameters, tuning in the proposed circuit, the FO can be scaled up more flexibly than that of which depends only on tuning the filter parameters. The results from computer simulation and from the experiment employing a commercial transconductance IC: LM13700 demonstrate and confirm the workability of the proposed work.

2. METHOD OF VDTA

The proposed quadrature shadow oscillator employs the VDTAs as the main active components to realize a filter cell and the external amplifier. Basic properties of the VDTA are briefly discussed. The VDTA is well known as a universal active building block with a pair of input terminals: V_p and V_N ; and three current output terminals: Z, X+, and X-. The symbol and the internal detail of the VDTA is depicted, respectively, in Figures 1(a) and 1(b). The matrix-representation in (1) shows the relationship among the parameters at all terminals. Meanwhile, the transconductances g_{m1} and g_{m2} of the device can be varied by adjusting the dc bias currents. The input-output relationship of the VDTA is described as (1).

$$\begin{bmatrix} I_Z \\ I_{X+} \\ I_{X-} \end{bmatrix} = \begin{bmatrix} g_{m1} & -g_{m1} & 0 \\ 0 & 0 & g_{m2} \\ 0 & 0 & -g_{m2} \end{bmatrix} \begin{bmatrix} V_{Vp} \\ V_{VN} \\ V_Z \end{bmatrix} \quad (1)$$

The transconductance of the VDTA can be approximated as $g_{m1} \approx (g_3 + g_4)/2$ and $g_{m2} \approx (g_5 + g_8)/2$. The transconductance value g_i of the i^{th} transistor can be found as (2):

$$g_i = \sqrt{I_{Bi} \mu_i C_{OX} \left[\frac{W}{L} \right]_i} \tag{2}$$

where μ_i is the mobility carrier of the NMOS and PMOS transistor; C_{OX} is the gate-oxide capacitance per unit area; W is the effective channel width; L is the effective channel length; I_{Bi} is the bias current of the i^{th} transistor.

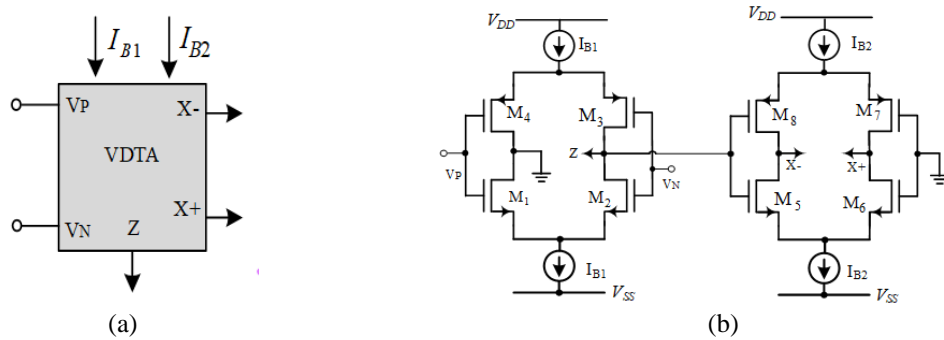


Figure 1. VDTA (a) symbolic diagram and (b) circuit diagram-CMOS implemented

3. PROPOSED QUADRATURE SHADOW OSCILLATOR

The proposed quadrature shadow oscillator can be implemented as shown in Figure 2. The circuitry is simple and requires a small number of components, i.e., two VDTAs, two resistors, and two grounded capacitors. VDTA 2 performs the filter cell which gives the bandpass and lowpass response having the following transfer functions.

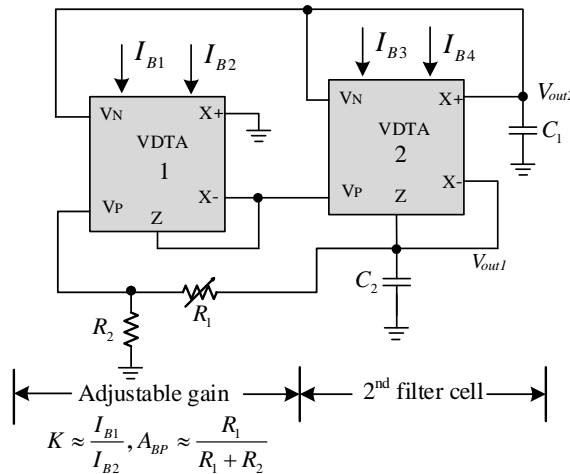


Figure 2. Schematic diagram of the proposed quadrature shadow oscillator

$$T_{BP}(s) = \frac{sC_1g_{m3}}{C_1C_2s^2 + sC_1g_{m4} + g_{m3}g_{m4}} \tag{3}$$

$$T_{LP}(s) = \frac{g_{m3}g_{m4}}{C_1C_2s^2 + sC_1g_{m4} + g_{m3}g_{m4}} \tag{4}$$

Meanwhile VDTA 1 realizes the external amplifier with the following gain K .

$$K \approx \frac{g_{m1}}{g_{m2}} \approx \frac{I_{B1}}{I_{B2}} \quad (5)$$

The compound resistor R_1 and R_2 provides the attenuator gain A_{BP} , were

$$A_{BP} \approx \frac{R_1}{R_2 + R_1} \quad (6)$$

Routine analysis results in the following characteristic equation.

$$C_1 C_2 s^2 + s(C_1 g_{m4} - C_1 K A_{BP} g_{m3}) + (1 + K) g_{m3} g_{m4} = 0 \quad (7)$$

Using the Barkhuizen oscillation criteria, the associated FO and CO are found, respectively as (8) and (9).

$$\omega_{ocs} = \sqrt{1 + K} \cdot \sqrt{\frac{g_{m3} g_{m4}}{C_1 C_2}} = \sqrt{1 + K} \cdot \omega_0 \quad (8)$$

$$A_{BP} = \frac{R_1}{R_1 + R_2} = \frac{g_{m4}}{g_{m3} K} \quad (9)$$

From (8), the FO can be adjusted via the external gain K , g_{m3} and g_{m4} . However, to follow the shadow filter concept, it is intended to tune the FO via only the external gain, i.e., adjusting the dc bias currents I_{B1} and I_{B2} of VDTA1. In the filter cell, the values of the bias currents and the capacitors are maintained as constants.

In addition, from (8), the FO of the shadow oscillator is the product of factor $\sqrt{1 + K}$ and ω_0 therefore the FO can be scaled up even if the same filter parameters are of use. Moreover, from (8) and (9), orthogonal controlling the FO and CO is evident. The CO can be set up by choosing the appropriate value of two resistors which should be equal to $g_{m4}/(g_{m3} K)$. Assuming the high input impedance at the VDTA-Vp terminal, the gain A_{BP} can be approximated to $\frac{R_1}{(R_1 + R_2)}$.

It is convenient to set up the CO by keeping the dc bias currents of the filter to the same value, i.e., $I_{B3} = I_{B4}$. As a result, $g_{m3} \approx g_{m4}$, and the A_{BP} term is a reciprocal of the value K . It should be noted that K depending on the bias current of the VDTA is approximated to the ratio of I_{B1} and I_{B2} . Next, the relationship between the two outputs is found. According to Figure 2, the voltage outputs at the FO can be expressed as (10).

$$\frac{V_{out2}}{V_{out1}} = \frac{g_{m4}}{j\omega_{osc} C_1} \quad (10)$$

Obviously, the voltage outputs V_{out1} and V_{out2} have 90° phase differences at the operating frequency. Then substitution of (8) into (10), absolute ratio of both outputs at the FO can be found as (11).

$$\left| \frac{V_{out2}}{V_{out1}} \right| = \frac{1}{\sqrt{1+K}} \cdot \sqrt{\frac{g_{m4} C_2}{g_{m3} C_1}} \quad (11)$$

From (11), the output signal ratio at the FO depends on the external gain too. Then the sensitivities of the FO related to some important parameters can be found as (12).

$$\begin{aligned} S_K^{\omega_{osc}} &= \frac{1}{2} - \frac{1}{2(1+K)}, \\ S_{I_{B1}}^{\omega_{osc}} &= \frac{1}{2} - \frac{1}{2(1+\frac{I_{B1}}{I_{B2}})}, \\ S_{I_{B2}}^{\omega_{osc}} &= -\frac{1}{2} + \frac{1}{2(1+\frac{I_{B1}}{I_{B2}})}, \\ S_{A_{BP}}^{\omega_{osc}} &= S_{R_1}^{\omega_{osc}} = S_{R_2}^{\omega_{osc}} = 0 \end{aligned} \quad (12)$$

It is seen from (12), all the sensitivities of FO are acceptably less than unity.

4. ANALYSIS OF NON-IDEALITY IN VDTA

4.1. The effect of transconductance gain error

This section discusses the effect of non-ideality in the VDTA on the FO. A non-ideal VDTA due to the transconductance error can be modelled as represented by the following matrix.

$$\begin{bmatrix} I_Z \\ I_{X+} \\ I_{X-} \end{bmatrix} = \begin{bmatrix} \alpha_i g_{m1} & -\alpha_i g_{m1} & 0 \\ 0 & 0 & \beta_{ij} g_{m2} \\ 0 & 0 & -\beta_{ij} g_{m2} \end{bmatrix} \begin{bmatrix} V_{V_P} \\ V_{V_N} \\ V_Z \end{bmatrix} \quad (13)$$

where α_i and β_{ij} are the transconductance gain error factors with i being the VDTA number and j being the output of the VDTA. Brief analysis discovers that the effect of non-ideality on the FO can be found as (14).

$$\omega_{ocs} = \sqrt{\alpha_2 \beta_{2X+} \left(1 + \frac{\alpha_1}{\beta_{1X-}} K\right)} \cdot \sqrt{\frac{g_{m3} g_{m4}}{c_1 c_2}} \quad (14)$$

Clearly, the transconductance errors causes the FO to drift. The sensitivity of the FO is then computed, and the results show that all the related sensitivities are still not greater than unity.

$$\begin{aligned} S_K^{\omega_{osc}} &= S_{\alpha_1}^{\omega_{osc}} = \frac{1}{2} - \frac{1}{2\left(1 + \frac{\alpha_1 K}{\beta_{1X-}}\right)}, \\ S_{\beta_{1X-}}^{\omega_{osc}} &= -\frac{1}{2} + \frac{1}{2\left(1 + \frac{\alpha_1}{\beta_{1X-}}\right)}, \\ S_{\alpha_2}^{\omega_{osc}} &= S_{\beta_{2X+}}^{\omega_{osc}} = \frac{1}{2} \end{aligned} \quad (15)$$

4.2. The effect of parasitic impedance on the FO

To study the parasitic impedance effects, a non-ideal VDTA model that incorporates the parasitic impedances is considered. The VDTA has parasitic impedances at all terminals. These impedances are represented as virtual grounded resistors and capacitors as shown in Figure 3. In the filter section, the parasitic impedances can be shown in Figure 4.

In the amplifier section, the modified gains including the parasitic impedances can be written as (16).

$$K = \frac{g_{m1}}{g_{m2} + G_{1Z} + G_{2P} + C_{1Z} + C_{2P}} \quad (16)$$

The voltage transfer function of the filter can then be given as (17) and (18):

$$\frac{V_{out1}}{V_A} = \frac{(sC_1 + G'_P)g_{m3}}{D(s)} \quad (17)$$

$$\frac{V_{out2}}{V_A} = \frac{g_{m3}g_{m4}}{D(s)} \quad (18)$$

where $D(s) = (C_1 + C'_P)(C_2 + C''_P)s^2 + s\{(C_2 + C''_P)G'_P + (C_1 + C'_P)G''_P + g_{m4}(C_1 + C'_P)\} + G'_P G''_P + g_{m4}G'_P + g_{m3}g_{m4}$. From (17) and (18), the frequency oscillation can be found as (19):

$$\omega_{osc} = \sqrt{1 + \left[\frac{g_{m1}}{(G_{3Z} + G_{1N} + C_{3Z} + C_{1N})(g_{m2} + G_{1Z} + G_{2P} + C_{1Z} + C_{2P})} \right]} \omega_o \quad (19)$$

where

$$\omega_o = \sqrt{\frac{G'_P G''_P + g_{m4}G'_P + g_{m3}g_{m4}}{(C_1 + C'_P)(C_2 + C''_P)}}$$

Obviously, the circuit still maintains the oscillatory function but with the deviated FO due to the parasitic effects.

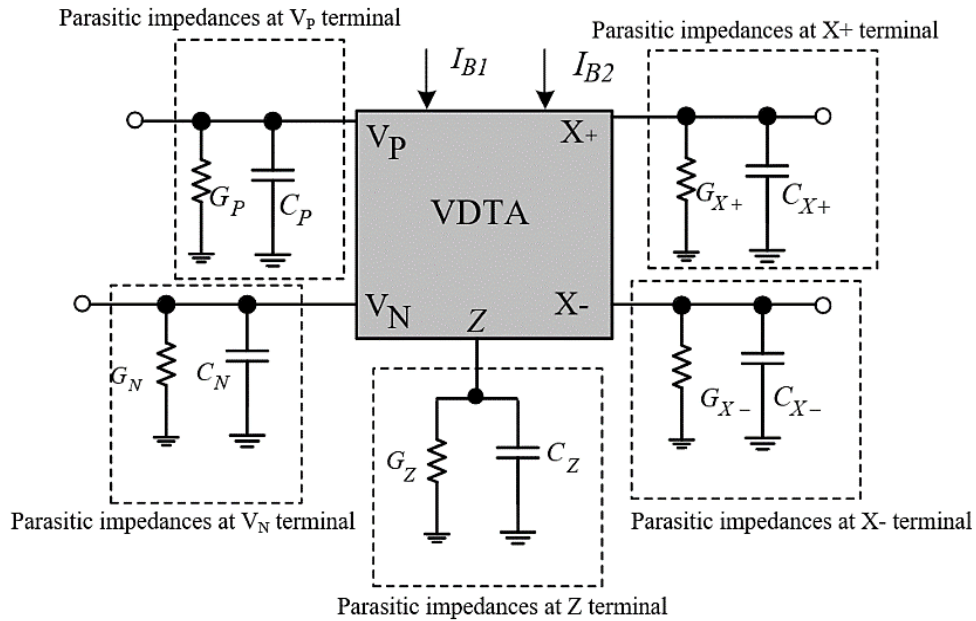


Figure 3. VDTA including parasitic impedances [35]

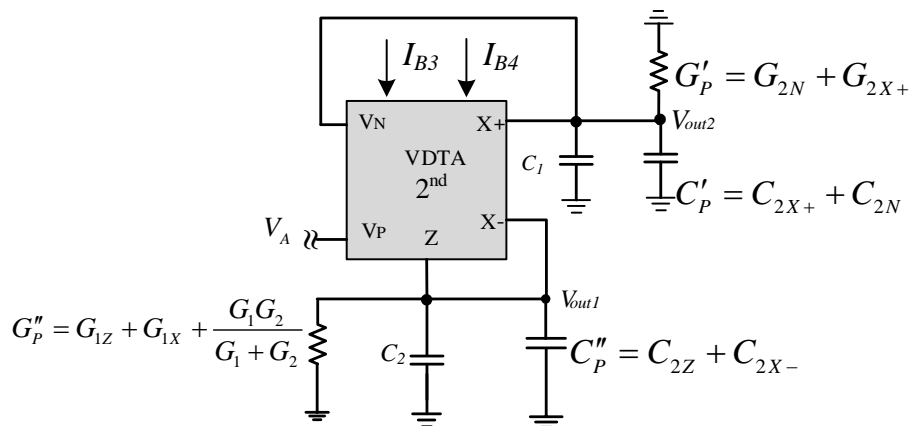


Figure 4. Filter cell with parasitic impedances

5. SIMULATION AND EXPERIMENTATION RESULTS

For evaluation, the proposed quadrature shadow oscillator is simulated using the TSMC 180 nm CMOS model parameters. The implementation of VDTAs employs the CMOS dimensions as those show in Table 1. All simulations use $\pm 1V$ power supplies. Firstly, the performance in the time-domain is investigated. For the filter section, $I_{B3} = I_{B4} = 50 \mu A$; $C_1 = C_2 = 0.3 \text{ nF}$; $A_{BP} = 0.7$ by choosing $R_1 = 10 \text{ k}\Omega$ and $R_2 = 4 \text{ k}\Omega$. Meanwhile the external gain $K = 7$ by setting $I_{B1} = 70 \mu A$ and $I_{B2} = 10 \mu A$. The simulation results of the time-domain responses of the two output voltages are demonstrated in Figures 5(a) and 5(b). It is clearly seen from the Figure 5 that both outputs can be self-oscillating as expected. Then Figure 6 depicts the two outputs in the steady-state within a short range of enlarged time-scale. Clearly, the proposed circuit generates two sinusoidal signals. In the figures, one has the amplitude of 80 mV_p and the other 33 mV_p and both having FO at 342 kHz with 90° phase difference.

Table 1. CMOS parameters for the VDTA-internal circuit [35]

Transistors	w(μm)	L(μm)
M_1, M_2, M_5, M_6	3.60	0.36
M_3, M_4, M_7, M_8	16.64	0.36

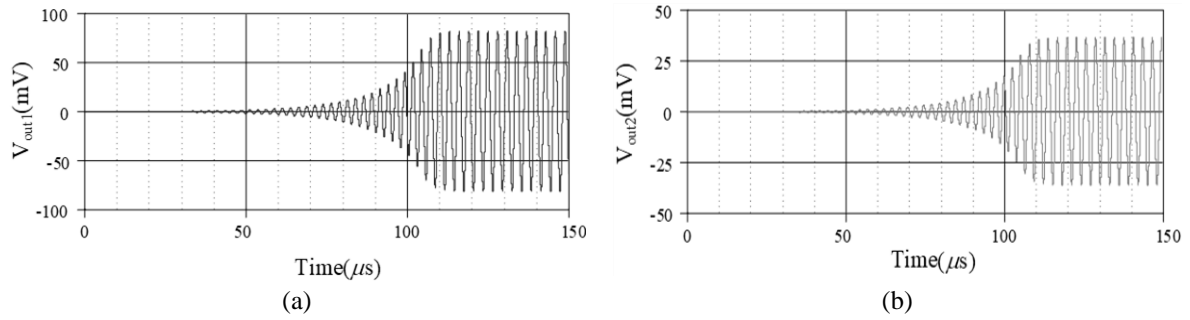


Figure 5. Time-domain responses (a) V_{out1} and (b) V_{out2}

Additionally, the frequency spectrum of the voltages in Figure 6 are demonstrated in Figure 7. From the spectrum, the fundamental frequency is distinctly situated at 342 kHz. The total harmonic distortions (THD) of V_{out1} and V_{out2} are found, respectively, as 6.04% and 1.93%. For verification of the 90° phase shift, the two outputs are plotted in the XY-plane and the results are demonstrated in Figure 8. Clearly, the desired 90° phase difference is obtained.

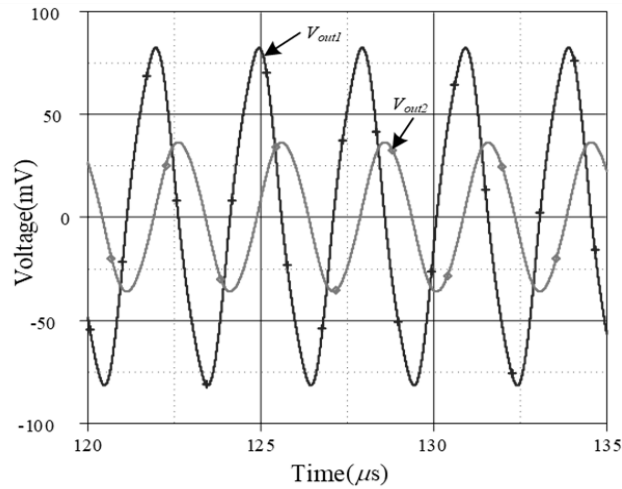


Figure 6. Steady-state responses of V_{out1} and V_{out2}

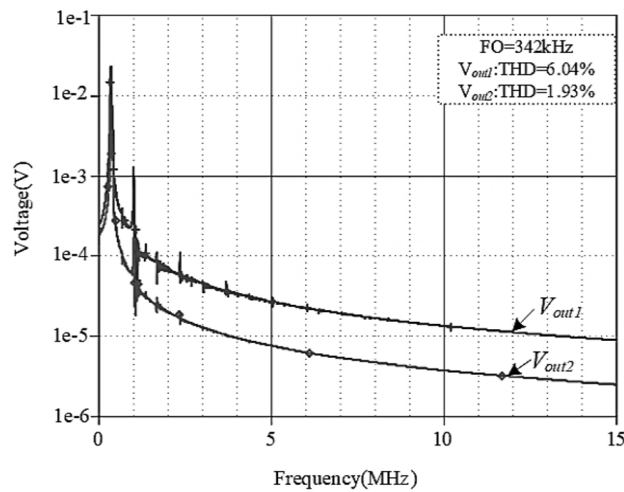


Figure 7. Frequency spectrum of the two outputs V_{out1} and V_{out2}

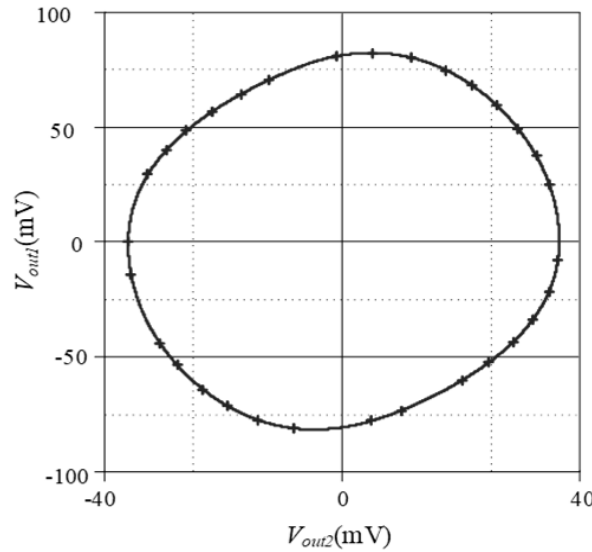


Figure 8. Lissajous curve of the two sinusoidal outputs

Besides, to explore the property of electronic tunability that does not disturb the filter cell, the proposed quadrature shadow oscillator is simulated and only the external gain K is varied from 1-10. This can be set by using $I_{B1} = 10$ to $100 \mu\text{A}$ and $I_{B2} = 10 \mu\text{A}$. Meanwhile, all the other parameters of the filter cell are fixed, i.e., $I_{B3} = I_{B4} = 50 \mu\text{A}$ and $C_1 = C_2 = 0.3 \text{ nF}$. The graph in Figure 9 shows the FO appropriately varies from 225 to 395 kHz relating to variation of the external gain K . The effect of various controlling gains on the phase difference between the two outputs are also simulated and the results are given in Figure 10.

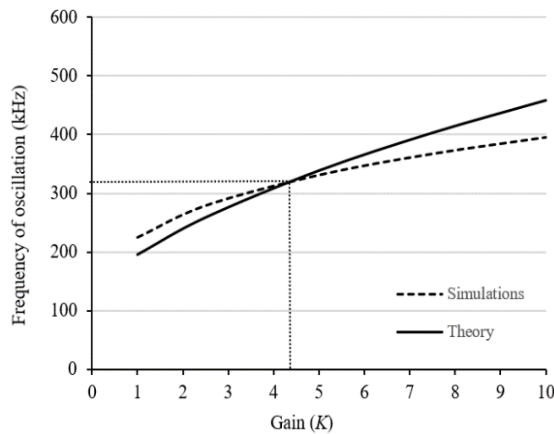


Figure 9. Frequency of oscillation obtained from varying the gain K ; $C_1 = C_2 = 0.3 \text{ nF}$

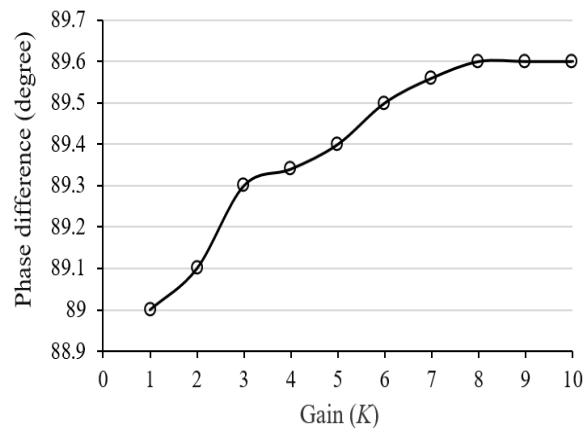


Figure 10. Phase differences between the two outputs due to variation of the gain K

The proposed circuit is then explored by the Monte Carlo analysis. In this simulation, the capacitor value deviates 5% with Gaussian distribution while the number of simulations is 100 run times and the gain $K=4$. The circuit parameters are set with $I_{B1} = 40 \mu\text{A}$, $I_{B2} = 10 \mu\text{A}$, $I_{B3} = I_{B4} = 50 \mu\text{A}$, $C_1 = C_2 = 0.3 \text{ nF}$. To ensure self-oscillations, the resistors are chosen as $R_1=3 \text{ k}\Omega$ and $R_2=3.45 \text{ k}\Omega$. Then the histograms of the FOs from the two outputs are shown in Figures 11(a) and 11(b). The histogram of the phase differences between the two outputs is also shown in Figure 11(c).

To confirm the workability, the proposed quadrature oscillator is further explored by actual circuit experiment. In the experiment, commercially available LM13700 operational transconductance amplifiers are employed as the main active elements. Then the schematic diagram is given in Figure 12. The circuit

construction on a breadboard is also shown in Figure 13. From the experiment, the parameters in the filter cell are such that the power supplies are set at ± 12 V, $C_1 = C_2 = 4.7$ μ F and the two transconductances are 440 μ A/V. The external gain is set to 5.7 by using $I_{B1} = 266$ μ A, $I_{B2} = 46$ μ A and $R_1 = 1.18$ k Ω and $R_2 = 10$ k Ω . The oscilloscope screen shown in Figure 14 demonstrates the two sinusoidal output signals, V_{out1} the marked trace having the amplitude of 84 mV and the unmarked V_{out2} having 60 mV of amplitude. The experiment results in the FO of about 34 kHz with a quadrature phase difference, whereas the theoretical value of the FO is 38 kHz. Then the two signals are plotted in the XY-mode as depicted in Figure 15. From the experiment, the information about the spectrum is also collected. Figure 16 shows the spectrum of the output voltage V_{out1} . The magnitude of the highest spectrum is greater than 50 dB comparing with the dominant harmonic in the vicinity.

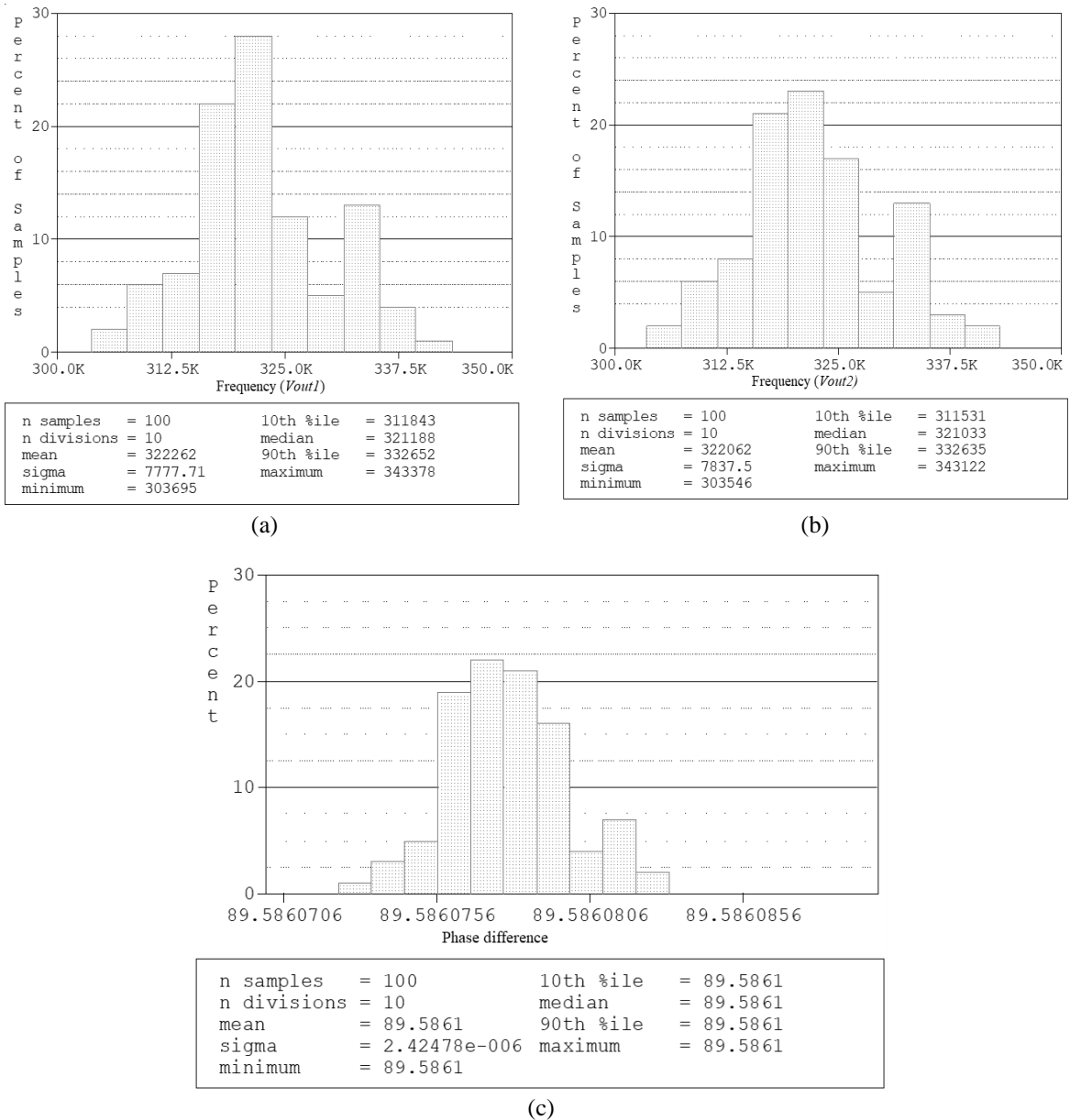


Figure 11. Histogram from the Monte-Carlo analysis with 5% deviation of capacitor (a) FO of V_{out1} , (b) FO of V_{out2} , and (c) phase differences

It is interesting to note that the simulation results demonstrate that the proposed circuit can produce sinusoidal signals with a quadrature phase-difference and the frequency of the oscillation can be controlled

through the circuit parameters. The value of g_m in the experimentation associated with the LM13700 can be approximated as about tenfold of the bias currents, i.e., $\approx 10I_B$ A/V. Meanwhile, in the simulation part using the same bias current, g_m is obtained as $233 \mu\text{A/V}$ which is smaller than that obtained in the experiment part. Hence, under the other same condition of gains and capacitors, the FO obtained from the experiment is larger than the FO in simulation part.

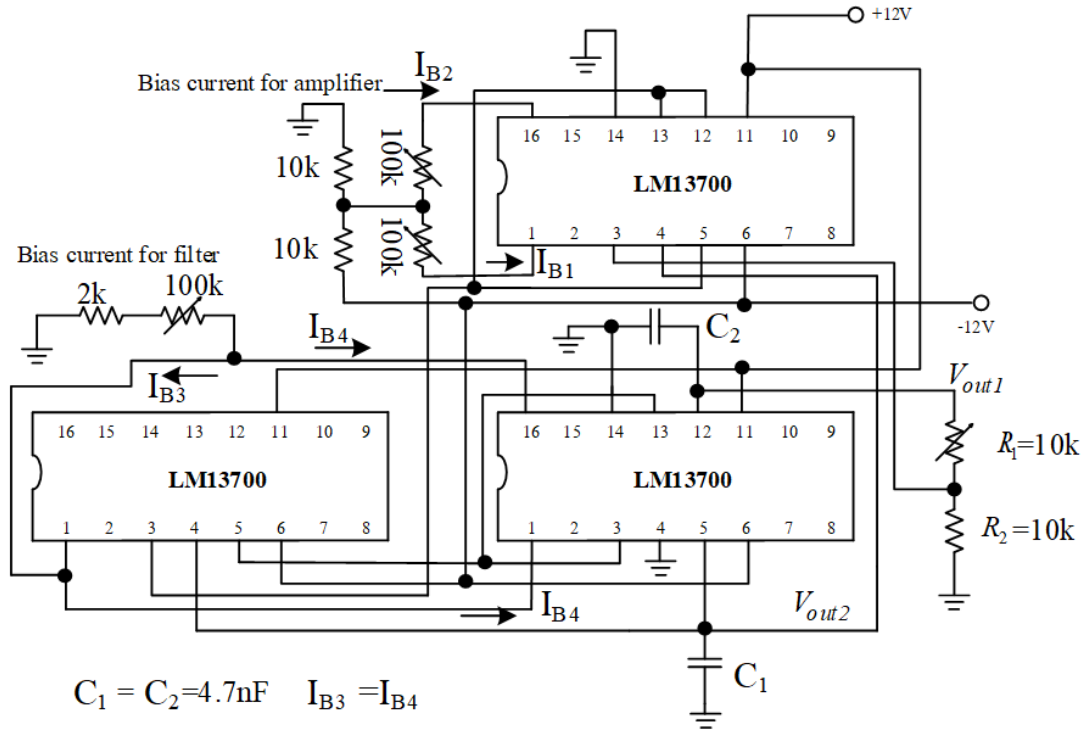


Figure 12. Schematic diagram for experimentation of the proposed shadow oscillator

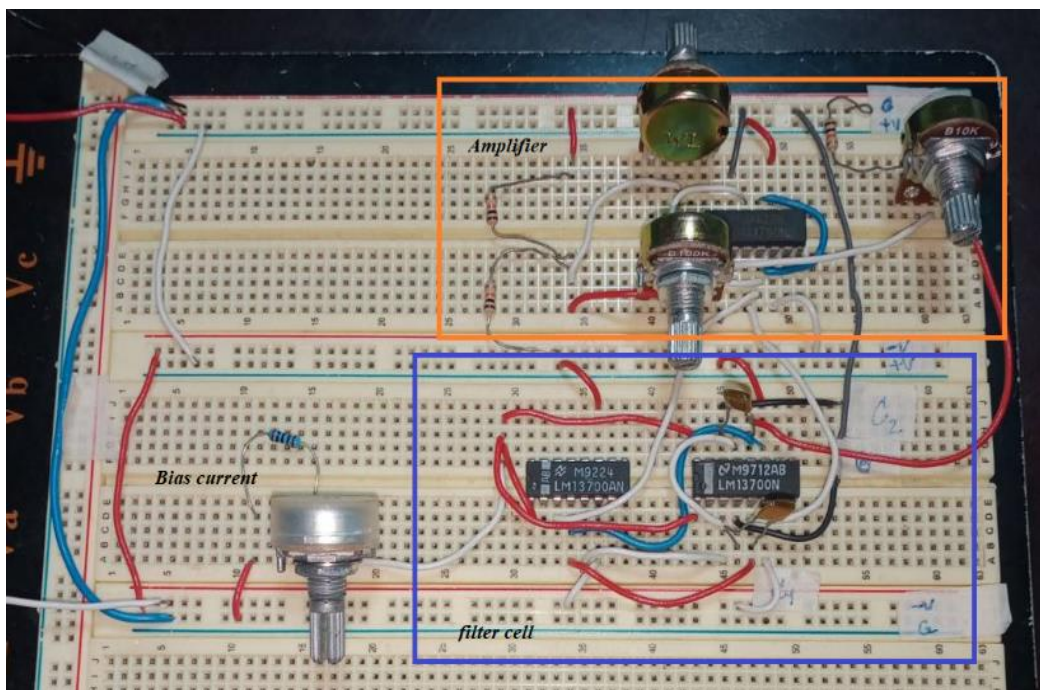


Figure 13. Experimental breadboard using the active components LM13700

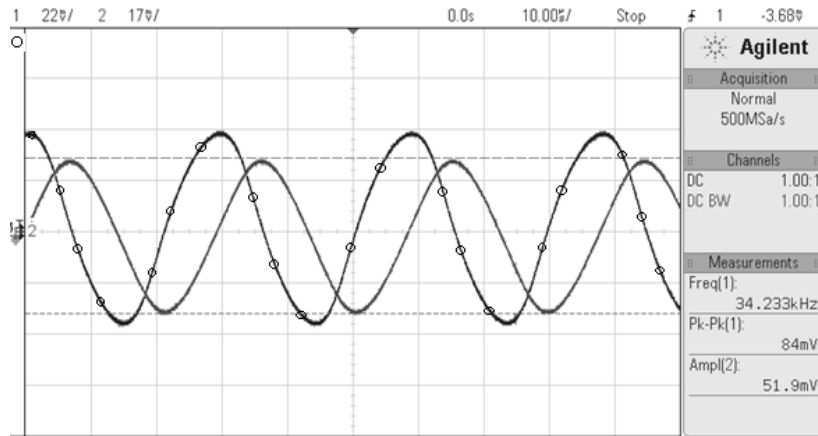


Figure 14. Experimental results showing the output voltages of the proposed quadrature shadow oscillator

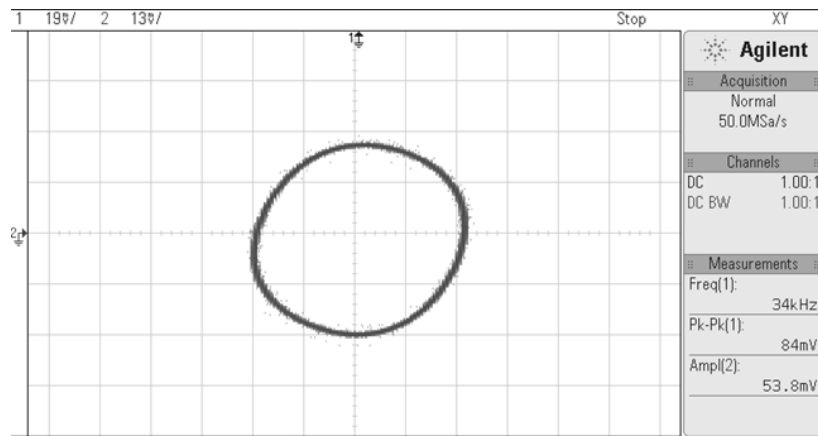


Figure 15. XY display of the voltage outputs from the experiment

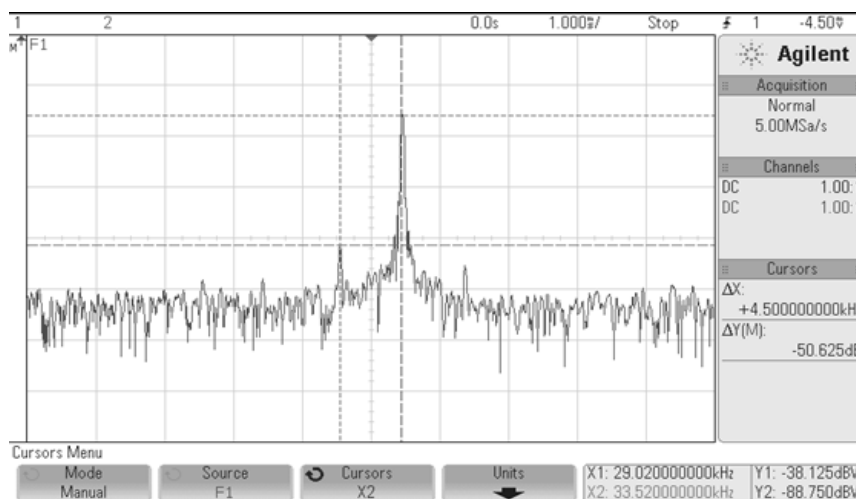


Figure 16. Experimental result about spectrum frequency measurement of V_{out}

6. PROPERTIES COMPARISON WITH PREVIOUS WORKS

For some little assessment among the various quadrature oscillators including the one having been proposed, a list of important characteristics is given in Table 2. Therefore, considering a number of aspects

given in the table, the proposed work obviously has many advantages worth further development. The features of the proposed work include being the quadrature and shadow mode of oscillators; small number of component-count; capacitors inside the implemented circuit are all grounded; the oscillator-characteristics are electronically tuned as well as orthogonally controlled.

Table 2. Important parameters of the previous oscillators and the proposed oscillators

Parameters	Ref [21]	Ref [32]	Ref [33]	Ref [34]	Proposed
Components	1VDTA+2C	1 Op-amp +2CFOA +7R+2C	2integrator +CCA+AGC	3VDTA+2C+2R	2VDTA+2C+2R
Grounded capacitors	✓	✗	✓	✓	✓
Shadow oscillator feature	✗	✓	✓	✓	✓
Quadrature phase output	✓	✗	N/A	✓	✓
Electronical tuning	✓	✗	✓	✓	✓
Type of control	Independent	Orthogonal	N/A	N/A	Orthogonal
Sensitivity	Less than unity	N/A	N/A	Less than unity	Less than unity
FO depend on the external gain	✗	✓	✗	✓	✓
Expansion of FO	✗	N/A	✗	✓	✓
Feedback signal	BP	N/A	BP	BP+LP	BP+LP

7. CONCLUSION

A new design of quadrature shadow oscillator is proposed. The design presents a few merits as the condition of oscillation and the frequency of oscillation can be independently controlled without disturbing the internal filter cell. To control the CO and the FO is also in orthogonal mode. As the circuit implementation consists of two VDTAs and a few passive components, the FO is tuned via the dc bias current of the external amplifier based on the VDTA realization. Another advantage of the proposed design is that the range of the FO can be easily extended as compared to the previous classical version due to the term $\sqrt{1+K}$, where K is the external amplifier gain. This feature is then suitable for applications such as fine-tuning and the error compensation of mismatch parameters within filter cells after the completion of the integrated-circuit process. Finally, the validity of the proposed work is well-confirmed by both computer simulation and circuit experiment.





REFERENCES

- [1] L. W. Couch, *Digital and analog communication systems*. New Jersey, US: Prentice Hall, One Lake Street, 2013.
- [2] D. Zheng, S. Zhang, S. Wang, C. Hu, and X. Zhao, "A capacitive rotary encoder based on quadrature modulation and demodulation," *IEEE Transactions on Instrumentation and Measurement*, vol. 64, no. 1, pp. 143–153, Jan. 2015, doi: 10.1109/TIM.2014.2328456.
- [3] S.-F. Wang, H.-P. Chen, Y. Ku, and P.-Y. Chen, "A CFOA-based voltage-mode multifunction biquadratic filter and a quadrature oscillator using the CFOA-based biquadratic filter," *Applied Sciences*, vol. 9, no. 11, Jun. 2019, doi: 10.3390/app9112304.
- [4] F. Yucel and E. Yuce, "Supplementary CCII based second-order universal filter and quadrature oscillators," *AEU - International Journal of Electronics and Communications*, vol. 118, May 2020, doi: 10.1016/j.aeue.2020.153138.
- [5] S.-F. Wang, H.-P. Chen, Y. Ku, and M.-X. Zhong, "Voltage-mode multifunction biquad filter and its application as fully-uncoupled quadrature oscillator based on current-feedback operational amplifiers," *Sensors*, vol. 20, no. 22, Nov. 2020, doi: 10.3390/s20226681.
- [6] S. S. Borah, A. Singh, M. Ghosh, and A. Ranjan, "Electronically tunable higher-order quadrature oscillator employing CDBA," *Microelectronics Journal*, vol. 108, Feb. 2021, doi: 10.1016/j.mejo.2020.104985.
- [7] S.-F. Wang, H.-P. Chen, Y. Ku, and M.-X. Zhong, "Analytical synthesis of high-pass, band-pass and low-pass biquadratic filters and its quadrature oscillator application using current-feedback operational amplifiers," *IEEE Access*, vol. 9, pp. 13330–13343, 2021, doi: 10.1109/ACCESS.2021.3050751.
- [8] M. Ghosh, S. S. Borah, A. Singh, and A. Ranjan, "Third order quadrature oscillator and its application using CDBA," *Analog Integrated Circuits and Signal Processing*, vol. 107, no. 3, pp. 575–595, Jun. 2021, doi: 10.1007/s10470-021-01812-3.
- [9] M. Dogan and E. Yuce, "A first-order universal filter including a grounded capacitor and two CFOAs," *Analog Integrated Circuits and Signal Processing*, vol. 112, no. 2, pp. 379–390, Aug. 2022, doi: 10.1007/s10470-022-02021-2.
- [10] V. Stornelli *et al.*, "A new VCII application: sinusoidal oscillators," *Journal of Low Power Electronics and Applications*, vol. 11, no. 3, Jul. 2021, doi: 10.3390/jlpeal1030030.
- [11] S. Tiwari and T. S. Arora, "Two new voltage-mode sinusoidal quadrature oscillators employing second-generation voltage conveyors," *IETE Journal of Research*, pp. 1–14, Nov. 2022, doi: 10.1080/03772063.2022.2138579.
- [12] T. S. Arora and A. K. Singh, "A new voltage mode sinusoidal quadrature oscillator employing second generation voltage conveyor," *AEU - International Journal of Electronics and Communications*, vol. 154, Sep. 2022, doi: 10.1016/j.aeue.2022.154304.
- [13] T. S. Arora and S. Gupta, "A new voltage mode quadrature oscillator using grounded capacitors: An application of CDBA," *Engineering science and technology, an international journal*, vol. 21, no. 1, pp. 43–49, 2018.
- [14] R. Bhagat, D. R. Bhaskar, and P. Kumar, "Quadrature sinusoidal oscillators using CDBAS: new realizations," *Circuits, Systems, and Signal Processing*, vol. 40, no. 6, pp. 2634–2658, Jun. 2021, doi: 10.1007/s00034-020-01603-7.
- [15] R. Pandey, N. Pandey, G. Komanapalli, and R. Anurag, "OTRA based voltage mode third order quadrature oscillator," *International Scholarly Research Notices*, 2014.



- [16] B. C. Nagar and S. K. Paul, "Voltage mode third order quadrature oscillators using OTRAs," *Analog Integrated Circuits and Signal Processing*, vol. 88, no. 3, pp. 517–530, Sep. 2016, doi: 10.1007/s10470-016-0781-6.
- [17] G. Komanapalli, N. Pandey, and R. Pandey, "New realization of third order sinusoidal oscillator using single OTRA," *AEU - International Journal of Electronics and Communications*, vol. 93, pp. 182–190, Sep. 2018, doi: 10.1016/j.aeue.2018.06.005.
- [18] D. V. Kamath, "OTA based current-mode sinusoidal quadrature oscillator circuits," *International Journal of System Modeling and Simulation*, vol. 1, no. 1, pp. 1–6, 2016.
- [19] S.-F. Wang, H.-P. Chen, Y. Ku, and C.-L. Lee, "Versatile voltage-mode biquadratic filter and quadrature oscillator using four OTAs and two grounded capacitors," *Electronics*, vol. 9, no. 9, Sep. 2020, doi: 10.3390/electronics9091493.
- [20] M. K. Jain and A. Singh, "Novel active-c voltage-mode quadrature oscillator realization employing CCCIs," *International Journal of Integrated Engineering*, vol. 14, no. 4, pp. 332–338, 2022.
- [21] K. Banerjee, D. Singh, and S. K. Paul, "Single VDTA based resistorless quadrature oscillator," *Analog Integrated Circuits and Signal Processing*, vol. 100, no. 2, pp. 495–500, Aug. 2019, doi: 10.1007/s10470-019-01480-4.
- [22] R. Sotner, J. Jerabek, N. Herencsar, and J. Petrzela, "Methods for extended tunability in quadrature oscillators based on enhanced electronic control of time constants," *IEEE Transactions on Instrumentation and Measurement*, vol. 67, no. 6, pp. 1495–1505, Jun. 2018, doi: 10.1109/TIM.2018.2799058.
- [23] M. Atasoyu, B. M. Metin, H. Kuntman, and N. Herencsar, "New current-mode class 1 frequency-agile filter for multi protocol GPS application," *Elektronika ir Elektrotechnika*, vol. 21, no. 5, pp. 35–39, Oct. 2015, doi: 10.5755/j01.eee.21.5.13323.
- [24] F. Khateb, W. Jaikla, T. Kulej, M. Kumngern, and D. Kubánek, "Shadow filters based on DDCC," *IET Circuits, Devices & Systems*, vol. 11, no. 6, pp. 631–637, Nov. 2017, doi: 10.1049/iet-cds.2016.0522.
- [25] D. Nand and N. Pandey, "New configuration for OFCC-based CM SIMO filter and its application as shadow filter," *Arabian Journal for Science and Engineering*, vol. 43, no. 6, pp. 3011–3022, Jun. 2018, doi: 10.1007/s13369-017-3058-1.
- [26] P. Huaihongthong *et al.*, "Single-input multiple-output voltage-mode shadow filter based on VDDAs," *AEU - International Journal of Electronics and Communications*, vol. 103, pp. 13–23, May 2019, doi: 10.1016/j.aeue.2019.02.013.
- [27] D. Singh and S. K. Paul, "Realization of current mode universal shadow filter," *AEU - International Journal of Electronics and Communications*, vol. 117, Apr. 2020, doi: 10.1016/j.aeue.2020.153088.
- [28] P. Prakash, Y. Srivastava, S. Kumar, and A. K. Singh, "Implementation of a shadow filter using CFCC," in *2021 2nd International Conference for Emerging Technology (INCET)*, May 2021, pp. 1–5, doi: 10.1109/INCET51464.2021.9456361.
- [29] S. D. Pathak, A. Luitel, S. Singh, and R. Pandey, "Second generation voltage conveyor II based shadow filter," in *2021 2nd International Conference for Emerging Technology (INCET)*, May 2021, pp. 1–5, doi: 10.1109/INCET51464.2021.9456370.
- [30] B. Metin, Y. Basaran, and O. Cicekoglu, "MOSFET-C current mode filter for secure communication applications," *AEU - International Journal of Electronics and Communications*, vol. 143, Jan. 2022, doi: 10.1016/j.aeue.2021.154017.
- [31] S. Buakaew and C. Wongtaychatham, "Boosting the quality factor of the shadow bandpass filter," *Journal of Circuits, Systems and Computers*, vol. 31, no. 14, Sep. 2022, doi: 10.1142/S0218126622502486.
- [32] M. T. Abuelma'atti and N. Almutairi, "A novel shadow sinusoidal oscillator," *International Journal of Electronics Letters*, vol. 5, no. 3, pp. 291–302, Jul. 2017, doi: 10.1080/21681724.2016.1209569.
- [33] F. J. Rubio, M. A. Dominguez, R. Perez-Aloe, J. M. Carrillo, and J. F. Duque-Carrillo, "Current-mode electronically-tunable sinusoidal oscillator based on a shadow bandpass filter," in *2022 18th International Conference on Synthesis, Modeling, Analysis and Simulation Methods and Applications to Circuit Design (SMACD)*, Jun. 2022, pp. 1–4, doi: 10.1109/SMACD55068.2022.9816315.
- [34] S. Buakaew and N. Atiwongsangthong, "Adjustable quadrature shadow sinusoidal oscillator," in *2022 8th International Conference on Engineering, Applied Sciences, and Technology (ICEAST)*, 2022, pp. 42–45, doi: 10.1109/ICEAST55249.2022.9826333.
- [35] A. Yeşil, F. Kaçar, and H. Kuntman, "New simple CMOS realization of voltage differencing transconductance amplifier and its RF filter application," *Radioengineering*, vol. 20, no. 3, pp. 632–637, 2011.

BIOGRAPHIES OF AUTHORS



Seangrawee Buakaew     earned a PhD in Electrical Engineering from King Mongkut's Institute of Technology Ladkrabang (KMITL) in Thailand. She is also a full-time lecture in Department of Electronics Engineering, KMITL. Her research focuses on analog circuit design, active filter, analog oscillator, circuit design in low voltage, circuit applications in instrumentation, and control systems. She can be contacted at email: seangrawee.to@kmitl.ac.th.



Chariya Wongtaychatham     received her bachelor and master degrees degree from King Mongkut's Institute of Technology Ladkrabang, Thailand. She also received PhD in Electrical Engineering from Wichita state university, Kansas, USA. Presently, she is an associate professor at the Department of Electronics Engineering, KMITL, Thailand. Her research fields of interest include analog circuit design and control system engineering. She can be contacted at email: chariya.wo@kmitl.ac.th.